Tikrit Journal of Engineering Sciences (2022) 29 (3): 49-58
DOI: http://doi.org/10.25130/tjes.29.3.6

IRAQI Academic Scientific Journals

ISSN: 1813-162X (Print); 2312-7589 (Online)

Tikrit Journal of Engineering Sciences

available online at: http://www.tj-es.com

TJES Tikrit Journal of Engineering Sciences

Theoretical Comparison of Characteristics between Elliptical and Conventional Hydrodynamic Journal Bearing

Ibrahem Ali Muhsin *, **Diyar Hassan Abdurrahman**

Mechanical Engineering Department, College of Engineering, Tikrit University, Tikrit, Iraq.

Keywords:

Tribology; Bearing; Elliptical Journal Bearing; Finite Difference Method; Bearing Performance

ARTICLE INFO

Article history:

Received	25 Apr. 2021
Accepted	30 Aug. 2022
Available online	11 Oct. 2022

Citation: Muhsin IA, Abdurrahman DH. Theoretical Comparison of Characteristics between Elliptical and Conventional Hydrodynamic Journal Bearing. Tikrit Journal of Engineering Sciences 2022; 29(3): 49- 58. **http://doi.org/10.25130/tjes.29.3.6**

ABSTRACT

In this research, two subjects are presented. The first one was, studying the effect of the ellipticity ratio on the bearing performance characteristics (flow rate, load number, power absorbed, and stiffness coefficients), where three different values of the ellipticity ratio (0.5, 1, and 1.5) were studied and the conventional bearing was considered as a reference for comparison with the elliptical bearing of different values of ellipticity ratio to demonstrate the effect of ellipticity ratio on the bearing performance, while the other aspect was, studying the effect of aspect ratio on the elliptical bearing performance. Three different values of aspect ratio (0.5, 1, and 1.5) were studied. This was achieved within the range (0.1 - 0.8) for the eccentricity ratio. The finite difference method was used to solve Reynold's equation numerically to obtain the pressure distribution on the bearing surface and then the bearing characteristics were computed. The computer program (Matlab R2015a) was used for solving the equations used in this study. From the results, it was observed that increasing the ellipticity ratio gives an increase in the flow rate values and a decrease in the (load number, power losses, Krr, Kss, |Krs| and Ksr) values, while, increasing the aspect ratio gives an increase in the (flow rate, power losses, Krr, Kss, |Krs| and Ksr) values and a decrease in the load number values. It was also observed that the elliptical bearing has a (higher flow rate, lower load capacity, and less power losses), than the conventional bearing. In addition, the elliptical bearing has higher principle stiffness coefficients (Krr and Kss) in the region ($n<0.41$) and ($n<0.66$), respectively, and lower cross-coupling stiffness coefficients (Krs and Ksr), than the conventional bearing.

* Corresponding author: E-mail: iboimu@tu.edu.iq, Mechanical Engineering Department, College of Engineering, Tikrit University, Tikrit, Iraq.

مقارنة نظرية بين خواص المسند الهيدروداينميكي التقليدي والمسند البيضوي

إبراهيم علي محسن قسم الهندسة الميكانيكية / كلية الهندسة / جامعة تكريت / العراق.
ديار حسن عبدالرحمن قسم الهندسة الميكانيكية / كلية الهندسة / جامعة تكريت / العراق.

الخلاصة

تم في احدى جوانب هذا البحث دراسة تأثير نسبة الإهليجية على خصائص أداء المسند (معدل التدفق، رقم التحميل، قدرة الممتصة ومعاملات النابضية)، حيث تمت دراسة ثلاث قيم مختلفة لنسبة الإهليجية (0.5، 1 و1.5) واعتبار المسند التقليدي كمرجع للمقارنة مع المسند البيضوي لقيم مختلفة لنسبة الإهليجية من أجل بيان تأثير نسبة الإهليجية على أداء المسند، بينما في الجانب الآخر تم دراسة تأثير نسبة (L/D) على أداء المسند البيضوي. تمت دراسة تأثير ثلاث قيم مختلفة لـ(L/D) (0.5، 1 و1.5). تم تحقيق ذلك ضمن المدى (0.1-0.8) من نسبة اللامركزية. تم استخدام طريقة الفروقات المحددة لحل معادلة رينولدز عدديا للحصول على توزيع الضغط على سطح المسند ثم تم حساب خصائص المسند. تم استخدام البرنامج الحاسوبي (Matlab R2015a) لحل المعادلات المستخدمة في هذه الدراسة. أظهرت النتائج، زيادة نسبة الإهليجية تزيد من قيم معدل التدفق وتخفض من قيم (رقم التحميل، خسائر القدرة، Krr، Kss، Krs|| وKsr) بينما زيادة نسبة (L/D) تزيد من قيم (معدل التدفق، خسائر القدرة، Krr، Kss، Krs|| وKsr) وتنخفض قيم رقم التحميل. ويلاحظ أيضا، أن المسند البيضوي يمتلك معدل تدفق أعلى، سعة تحميل أقل وفقد أقل للقدرة مقارنة بالمسند التقليدي. ويظهر أيضا أن المسند البيضوي يمتلك معاملات النابضية الأساسية (Krr وKss) أعلى من المسند التقليدي ضمن المدى (n<0.41) و (n<0.66) من نسبة اللامركزية على التوالي، ومعاملات النابضية المرافقة (Krs وKsr) أقل من المسند التقليدي.

1. INTRODUCTION

The hydrodynamic journal bearing is an important element in most of the mechanical rotating parts, where it provides support for the rotating shafts axially or radially, and it consists of two or more parts arranged in a way that allows loading as well as the relative movement between them. The bearings are classified according to their principle of operation, fluid film bearings, rolling element bearings, and dry (or rubbing) bearings, and are widely used in machinery and equipment's. For example, high-speed pumps and turbines, auto motors, and all mechanical machines that contain rotating parts. The design of the hydrodynamic bearings requires careful attention as the dynamic behavior of the machine and both the static and dynamic characteristics of the bearing must be taken into account in the design process to ensure non-contact between the bearing and the shaft surfaces during rotation, reliable operation, safety and efficiency of the bearing and the provision of specific values of stiffness coefficients. The failure in the hydrodynamic bearings occurs by slip wear when motion starts or ends [1]. The elliptical journal bearing is one of the most common types of non-circular hydrodynamic journal bearings and is widely used in high-speed rotating machines and large turbines because it enhances journal stability (high resistance to whirl), reduces power loss and increases oil flow (as compared with the circular bearings), thus reducing bearing temperature [2], and it is also characterized by its ability to rotate in both directions [3]. W. A. Crosby and B. Chetti [4] presented a study that examined the static and dynamic characteristics of an elliptical bearing that is lubricated using a couple-stress fluid. The finite element method was used to solve the Reynolds equation numerically to obtain the oil film pressure distribution on the bearing surface. In this research they studied, the effect of eccentricity ratio on the static characteristics (load carrying capacity, attitude angle, and flow rate) and the effect of Somerfield number on the dynamic coefficients (stiffness k_{ij} and dampingC_{ij}) behavior. The obtained results showed that the bearing load capacity and oil flow are increased with the increase of eccentricity ratio while the attitude angle decreases with the increase of eccentricity ratio. As for the dynamic coefficients, the coefficients $(k_{xx}, k_{xy}, k_{yy}, C_{xx}, C_{yy})$ are increased with the increase of Somerfield number values while the coefficients (k_{yx}, C_{yx}) are decreased with the increase of Somerfield number values. Marco T. C. Faria [5] presented research that examined the dynamic performance of an elliptical bearing. The finite element method was used to solve Reynold's equation numerically and using a coordinate system in which the horizontal axis was (y) and the vertical was (x), and (L/D=1), where the effect of Somerfield number within the range (0.001-1) on the dynamic (stiffness and damping) coefficients were studied. The results showed that the stiffness and damping coefficients took their highest values at a low Somerfield number, the decrease in the Somerfield number is associated with the increase of the applied load on the bearing, which raises the values of the dynamic coefficients, then with an increase in Somerfield number and the dynamic coefficients significantly decrease. R. K. Awasthi and S. Sharma [6] investigated the effect of aspect ratio (L/D) on the performance

characteristics and stability of hydrodynamic bearings. The finite element method was used to solve Reynold's equation to obtain the oil pressure distribution and then to evaluate the static and dynamic characteristics. The results showed that attitude angle, stiffness coefficient S_{xz} and damping coefficients $C_{xx,}C_{xz},C_{zz},C_{zx}$ increase with the increase of the aspect ratio. While the stiffness coefficients S_{xx},S_{zx},S_{zz} increase with the decrease of the aspect ratio. In this paper, two subjects are presented, the first one is, studying the effect of the ellipticity ratio on the bearing performance characteristics (flow rate, load number, power absorbed, and stiffness coefficients), where three different values of the ellipticity ratio (0.5, 1 and 1.5) are studied and the conventional bearing is considered as a reference for comparison with the elliptical bearing of different values of to demonstrate the effect of on the bearing performance, while the other aspect is, studying the effect of three different values of aspect ratio (0.5, 1 and 1.5) on the elliptical bearing performance.

2.THEORETICAL ANALYSIS

The geometry of the elliptical journal bearing is shown schematically in Fig. 1. The elliptical bearing has two convergence zones [7]. The journal rotates in the bearing within a position determined by the eccentricity value and attitude angle [8].

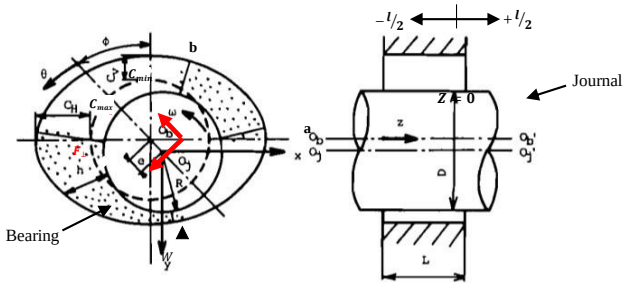

The Reynolds equation governing the oil film flow in the clearance space of a journal bearing is expressed as follows [9]:

$$\frac{1}{b^2}\frac{\partial}{\partial\theta}\left(\frac{h^3}{\mu}\frac{\partial P}{\partial\theta}\right)+\frac{\partial}{\partial z}\left(\frac{h^3}{\mu}\frac{\partial P}{\partial z}\right)=6\frac{U_o}{b}\frac{\partial h}{\partial\theta}+12\frac{\partial h}{\partial t} \quad \dots(1)$$

Simplifying Reynolds equation is based on the following assumptions:

1. Neglecting the body forces.
2. There is no slipping in the lubricant layers at the boundaries.
3. The pressure does not change radially.
4. The fluid's momentum forces are neglected compared with the forces of its viscosity.
5. The flow is laminar.
6. The oil is Newtonian.
7. Neglecting the oil temperature variation effect in the bearing performance
8. Non-compressive fluid.
9. The bearing is steady and the load is static.
10. Viscosity is constant.

2.1. Finite Difference Method

The finite difference technique is used for solving Reynold's equation numerically to obtain the pressure distribution on the bearing surface. The bearing surface is divided axially and circumferentially using grids, to apply the numerical solution [10].

Simplifying Reynolds equation according to the previous assumptions gives [11]:

$$\frac{\partial^2 P}{\partial\theta^2}+\frac{3}{h}\frac{\partial h}{\partial\theta}\frac{\partial P}{\partial\theta}+b^2\frac{\partial^2 P}{\partial Z^2}=6\frac{U_o\mu b}{h^3}\frac{\partial h}{\partial\theta} \quad \dots(2)$$

Assuming:

$$\left.\begin{aligned} C_1&=\frac{3}{h}\frac{\partial h}{\partial\theta}\\ C_2&=b^2\\ C_3&=6\frac{U_o\mu b}{h^3}\frac{\partial h}{\partial\theta}\end{aligned}\right\} \quad \dots(3)$$

Substituting $(C_1, C_2\ and\ C_3)$ in "Eq. (2)" gives:

$$\frac{\partial^2 P}{\partial\theta^2}+C_1\frac{\partial P}{\partial\theta}+C_2\frac{\partial^2 P}{\partial Z^2}=C_3 \quad \dots(4)$$

The first and second derivatives of the pressure $(P_{i,j})$ in the circumferential direction $\left(\frac{\partial P}{\partial\theta},\frac{\partial^2 P}{\partial\theta^2}\right)$ and the second derivative of the pressure in the axial direction $\left(\frac{\partial^2 P}{\partial Z^2}\right)$ are given respectively by:

$$\left.\frac{\partial P}{\partial\theta}\right)_{i,j}=\frac{P_{i+1,j}-P_{i-1,j}}{2\left(2\pi/_{m-1}\right)} \quad \dots(5)$$

$$\left.\frac{\partial^2 P}{\partial\theta^2}\right)_{i,j}=\frac{P_{i+1,j}-2P_{i,j}+P_{i-1,j}}{\left(2\pi/_{m-1}\right)^2} \quad \dots(6)$$

$$\left.\frac{\partial^2 P}{\partial z^2}\right)_{i,j}=\frac{P_{i.j+1}-2P_{i,j}+P_{i,j-1}}{\left(L/_{k-1}\right)^2} \quad \dots(7)$$

Substituting "Eq.s (5, 6 and 7)" in "Eq. (4)" gives:

$$\left(\frac{P_{i+1,j}-2P_{i,j}+P_{i-1,j}}{\left(2\pi/_{m-1}\right)^2}\right)+C_1\left(\frac{P_{i+1,j}-P_{i-1,j}}{2\left(2\pi/_{m-1}\right)}\right)+C_2\left(\frac{P_{i.j+1}-2P_{i,j}+P_{i,j-1}}{\left(L/_{k-1}\right)^2}\right)=C_3 \quad \dots(8)$$

Assuming:

$$\left.\begin{aligned} C_4&=\left(m-1/_{4\pi}\right)\\ C_5&=\left(m-1/_{2\pi}\right)^2\\ C_6&=\left(k-1/_{L}\right)^2\end{aligned}\right\} \quad \dots(9)$$

Substituting $(C_4, C_5\ and\ C_6)$ in "Eq. (8)" and rearranging it gives:

$$P_{i,j}=A_1P_{i+1.j}+A_2P_{i-1,j}+A_3P_{i,j+1}+A_3P_{i,j-1}-A_4 \quad \dots(10)$$

The film thickness of the elliptical bearing as shown in Fig. 1 is expressed by the following equation [7].

$$h=C_{min}+e\cos\theta+(C_{max}-C_{min})\,sin^2(\theta+\phi) \quad \dots(11)$$

The first derivative of (h) concerning (θ) is:

$$\frac{\partial h}{\partial\theta}=-\mathrm{e}\sin\theta+(C_{max}-C_{min})\sin2(\theta+\phi) \quad \dots(12)$$

2.2. Boundary Conditions

The boundary conditions of the pressure on the bearing surface in the circumferential and axial directions are as follow: The pressure boundaries in the circumferential direction for the conventional and elliptical bearings are:

1. **For conventional bearing:**
   $P = 0 \quad at \quad (\pi \le \theta \le 2\pi)$ ... **(13)**
2. **For elliptical bearing:**
   $$P = 0 \quad at \left(0 \le \theta \le \frac{\pi}{2} \; and \; \pi \le \theta \le \frac{3\pi}{2}\right) \quad \left.\begin{matrix} for \\ e = 0 \\ \phi = 0 \end{matrix}\right\} \quad \dots (14)$$

The pressure boundaries in the axial direction for both bearings (conventional and elliptical) are:

$$P = 0 \qquad at \qquad Z = \pm\frac{L}{2} \qquad \dots (15)$$

$$\frac{\partial p}{\partial z} = 0 \qquad at \qquad Z = 0 \qquad \dots (16)$$

2.3. Forces Analysis

The generated hydrodynamic pressure in the oil film between the bearing and the journal, generates a force on each element, and this force is analyzed into two components as shown in Fig.1, the first one is parallel to the line of centers, and the second one is perpendicular, and are given respectively as follows [11].

$$F_{\parallel_{i,j}} = a_e * P_{i,j} * \cos\theta_i \qquad \dots (17)$$

$$F_{\perp_{i,j}} = a_e * P_{i,j} * \sin\theta_i \qquad \dots (18)$$

The total parallel and perpendicular components of forces on the bearing surface are expressed respectively by:

$$F_{\parallel_t} = \sum_{i=1}^{m}\sum_{j=1}^{k}\left[F_{\parallel_{i,j}}\right] \qquad \dots (19)$$

$$F_{\perp_t} = \sum_{i=1}^{m}\sum_{j=1}^{k}\left[F_{\perp_{i,j}}\right] \qquad \dots (20)$$

Where:

$$a_e = \frac{A}{(m-1)(k-1)} \qquad \dots (21)$$

$$A = P_b * L \qquad \dots (22)$$

The bearing perimeter is [12]:

$$P_b = a\left[1.2\left(b/a\right)^2 + 1.1\left(b/a\right) + 4\right] \qquad \dots (23)$$

The load carrying capacity and the attitude angle are given respectively by:

$$W = \left(\left(F_{\parallel_t}\right)^2 + \left(F_{\perp_t}\right)^2\right)^{1/2} \qquad \dots (24)$$

$$\phi = \tan^{-1}\left[F_{\perp_t}/F_{\parallel_t}\right] \qquad \dots (25)$$

2.4.Static Characteristics of the Bearing

The static characteristics of the bearing (oil flow rate, load number, and power absorbed) are given respectively as follows [13]:

$$Q_r = \pi D L C_V \, n \, \overline{N} \qquad \dots (26)$$

$$L_N = \frac{4\bar{P}}{\mu\overline{N}}\left(C_V/D\right)^2\left(D/L\right)^2 \qquad \dots (27)$$

$$\psi = 2\pi\overline{N}\left[\left(\mu \, U_o \, L \, R^2/C_V\right)\left(2\pi/(1-n^2)^{1/2}\right)\right] + W * e\sin\phi \qquad \dots (28)$$

2.5. Stiffness Coefficients

The stiffness coefficients depend on the values of (attitude angle, eccentricity, and load-carrying capacity) and their variations due to the journal movement within the clearance space. These coefficients are calculated using the following equations [8]:

$$K_{rr} = \frac{\partial w}{\partial e}\cos\phi - W\frac{\partial\phi}{\partial e}\sin\phi \qquad \dots (29)$$

$$K_{ss} = \frac{W}{e}\cos\phi \qquad \dots (30)$$

$$K_{sr} = \frac{\partial w}{\partial e}\sin\phi + W\frac{\partial\phi}{\partial e}\cos\phi \qquad \dots (31)$$

$$K_{rs} = -\frac{W}{e}\sin\phi \qquad \dots (32)$$

Where the first subscript represents the direction of force and the second subscript the direction of displacement.

2.6. Computation Algorithm

Programming algorithm.

1. Assuming an initial value of the eccentricity ratio.
2. Assuming an initial value of the attitude angle.
3. Calculating the oil film thickness at each node on the bearing surface using "Eq. (11)".
4. Calculating the pressure value at each node by solving Reynolds "Eq. (10)".
5. The following convergence criteria $\left[\left|\frac{P_{(i,j)t} - P_{(i,j)t-1}}{P_{(i,j)t-1}}\right| \le 10^{-4}\right]$ is used to stop the iteration process and proceed forward otherwise go to step 4.
6. Calculating the total parallel component of force and perpendicular component of force using "Eq. (19 and 20)", respectively.
7. Calculating the attitude angle using "Eq. (25)".
8. Comparing ϕ_c with ϕ, if $[|\phi_c - \phi| \le 0.1]$ then move to the next step, otherwise, modify its initial value and return to step 2.
9. Calculating the total load carrying capacity for the bearing using "Eq. (24)".
10. Calculating the oil flow rate using "Eq. (26)".
11. Calculating the load number using "Eq. (27)".
12. Calculating the power absorbed using "Eq. (28)".
13. Calculating stiffness coefficients (K_{rr}, K_{ss}, K_{sr} and K_{rs}) using "Eq. (29, 30, 31 and 32)", respectively.
14. If the eccentricity ratio (n<0.8) returns to step1, otherwise move to the next step.
15. Printing the output results.

2.7.Flow Chart of the Elliptical Bearing Case

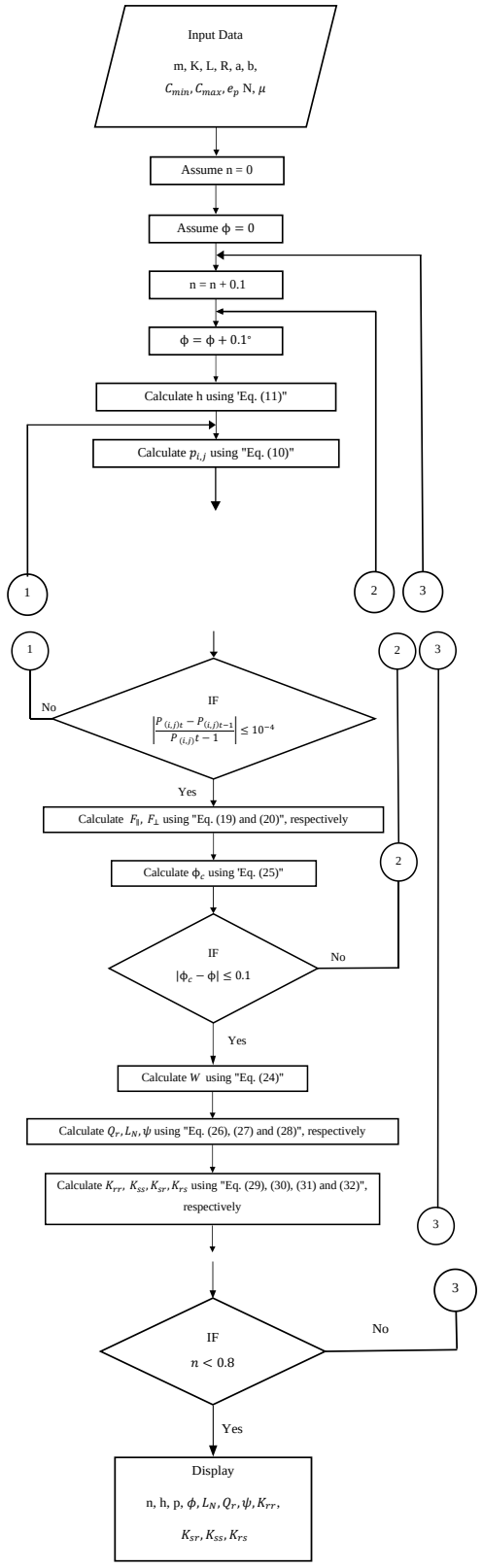

3.RESULTS AND DISCUSSION

It is useful to use the conventional bearing as a reference for comparison. The elliptical bearing has a different geometry than the conventional one. To demonstrate the ellipticity ratio effect on the static and dynamic characteristics, it is necessary to assess the static and dynamic characteristics of the conventional bearing first, then the elliptical bearing. Therefore, the computer program was designed to calculate both characteristics. The two bearings share most of the parameter's values presented in Table 1. The obtained results for the conventional bearing have been compared with the bearing studied by [14], and the comparison results are presented in Fig. 2. It is clear that they have similar behavior (static and dynamic characteristics). In addition, this proves the validity of this work results.

Table1. Bearing parameter values used calculation.

Symbols	Definition	Values Used in the Current Study	Units
D	Journal diameter	0.05	m
C_{min}/R	Clearance-radius ratio	0.0016	-
C_{min}	Vertical radial clearance	4×10^{-5}	m
μ	Dynamic viscosity of the lubricant	3×10^{-3}	$Pa.s$
e_p	Ellipticity ratio	0.5, 1 and 1.5	-
L/D	Aspect ratio	0.5, 1 and 1.5	-
N	Journal speed	5000	$r.p.m$

To prove the validity of the obtained results from the computer program for the elliptical bearing, therefore, it is compared with other researchers' results. Static and dynamic characteristics of this bearing were compared with those researchers' results and it was found in good agreement with slight differences due to the variation of the design and operational parameters values. Fig.3 shows the variation of load carrying capacity (for elliptical bearing) with the eccentricity ratio for the current study and Ref. [15]. Fig. 4 shows the variation of the oil flow rate with the eccentricity ratio for different values of the ellipticity ratio. It is clear that the relation between oil flow rate and eccentricity ratio is linearly proportional for both, the conventional bearing and the elliptical bearing of any value of ellipticity ratio, and increasing the ellipticity ratio value causes an increase in the flow rate values. It is also clear that the conventional bearing gave the lowest value of flow rate than the elliptical bearing of any value of ellipticity ratio. The flow rate for the elliptical bearing is higher than that of the conventional, this is justified by the higher film thickness value for the first compared with the

second in the divergence regions, and this droop down the bearing temperature [2]. Fig. 5 shows the variation of load number with the eccentricity ratio of the conventional bearing and the elliptical bearing of any ellipticity ratio value. Referring to this figure, it is clear that, the load number value increases with an increase in the eccentricity ratio value for both, the conventional bearing and the elliptical bearing of any value of ellipticity ratio and the relation between load number and ellipticity ratio is inverse proportional. It is also clear that the conventional bearing gave the highest value of load number than the elliptical bearing of any value of ellipticity ratio. As a result of this negative effect of the ellipticity ratio on the load number value, therefore, using low ellipticity ratios is the closest one to the conventional bearing regarding the loading number, and always the conventional bearing has a higher load capacity than the elliptical bearing [16]. Moreover, this is considered a penalty for improving stability, as assumed to be. Fig. 6 shows the variation of power losses with eccentricity ratio for different values of ellipticity ratio. Referring to this figure, it is clear that, increasing the eccentricity ratio value causes an increase in power loss values for both, the conventional bearing and the elliptical bearing of any value of the ellipticity ratio. It is noted that for the elliptical bearing, all ellipticity ratio values gave very close values to each other and the conventional bearing gave the highest values of power losses. Generally speaking, the elliptical bearing of any ellipticity ratio gives fewer power losses compared with the conventional bearing [2]. Fig. 7 shows the variation of stiffness coefficient Krr with eccentricity ratio for different values of ellipticity ratio. This figure shows that increasing the eccentricity ratio value causes an increase in the Krr values for both, the conventional bearing and the elliptical bearing of any value of ellipticity ratio, and increasing the ellipticity ratio value causes a decrease of Krr values, and the conventional bearing gave the highest values of Krr than the elliptical bearing of any value of ellipticity ratio, in the region($n > 0.41$). Fig. 8 shows the variation of stiffness coefficient Krs with eccentricity ratio for different values of ellipticity ratio. This figure shows that the relation between (Krs) and eccentricity ratio is inverse proportional for both, the conventional bearing and the elliptical bearing of any value of ellipticity ratio and increasing the ellipticity ratio value cause a decrease in the Krs (absolute) values. It is also clear that the conventional bearing gave the highest (absolute) value of Krs than the elliptical bearing of any value of ellipticity ratio. Therefore, it could be concluded that using a high ellipticity ratio gives a positive influence on bearing stability. Fig. 9 shows the variation of stiffness coefficient Kss with eccentricity ratio for different values of ellipticity ratio. This figure shows that increasing the eccentricity ratio value causes an increase in Kss values for both, the conventional bearing and the elliptical bearing of any value of ellipticity ratio while increasing the ellipticity ratio value gives a negative influence (decreases Kss values). It is also clear that the elliptical bearing of any value of ellipticity ratio gave the highest values of Kss than the conventional bearing, in the region($n < 0.487$). It was noted that Kss curve for the conventional bearing suddenly changed its behavior (going up) and gave the highest values of Kss at the region($n > 0.487$). Fig. 10 shows the variation of stiffness coefficient Ksr with eccentricity ratio for different values of ellipticity ratio. Referring to this figure, it is clear that, increasing the eccentricity ratio value causes an increase in Ksr values for both, the conventional bearing and the elliptical bearing of any value of the ellipticity ratio. It is noted that Ksr values are close to each other in the region ($0 < n \leq 0.7$) for all ellipticity ratios. Generally speaking, the relation between Ksr and ellipticity ratio is inversely proportional. It is also clear that the conventional bearing has the highest values of Ksr than the elliptical bearing of any value of ellipticity ratio. Fig. 11 shows the variation of the oil flow rate with the eccentricity ratio for different values of the aspect ratio. Referring to this figure, it is clear, that the relation between oil flow rate and eccentricity ratio is linearly proportional to any value of aspect ratio and the relation between oil flow rate and aspect ratio is proportional. Fig. 12 shows the variation of load number with eccentricity ratio for different values of aspect ratio. This figure shows that, the relation between load number and eccentricity ratio is proportional to any value of aspect ratio, while the relation between load number and aspect ratio is inversely proportional. As a result of this negative effect of the aspect ratio on the load number value, therefore, using low aspect ratios increase the bearing load capacity. Fig. 13 shows the variation of power losses with eccentricity ratio for different values of aspect ratio. Referring to this figure, it is clear that, the relations between, power losses and eccentricity ratio for any aspect ratio value, power losses, and aspect ratio are proportional. Since the aspect ratio has a negative effect (increases power loss), thus using low aspect ratios is preferable since it decreases power losses and increases the load-carrying capacity (Fig. 4-3). This is justified as follows: having a large project area (L×D) gives a large shear rate of the oil layers hence increasing power losses. In addition, this means that elliptical bearing has the same trend as conventional bearing regarding power losses. Fig. 14 shows the variation of stiffness coefficient Krr with

eccentricity ratio for different values of aspect ratio. This figure shows that Krr values increase with an increase either in the eccentricity ratio (of any value of aspect ratio) or in the aspect ratio. So it may be concluded that increasing the aspect ratio improves bearing stability. These results are in a good agreement with the results of [17]. Fig. 15 shows the variation of stiffness coefficient Krs with eccentricity ratio for different values of aspect ratio. This figure shows that Krs values are decreased with the increase of eccentricity ratio value for the case of aspect ratio equal (0.5) only, while for the cases of aspect ratio equal (1 and 1.5), Krs values are increased in the range (0 – 0.5) for eccentricity ratio and then decreased. It is also clear that the relation between Krs and the aspect ratio is inversely proportional. These results are in a good agreement with the results of [17]. Fig. 16 shows the variation of stiffness coefficient Kss with eccentricity ratio for different values of aspect ratio. Referring to this figure, it is clear that, Kss values increase with an increase either in the eccentricity ratio (of any value of aspect ratio) or in the aspect ratio. These results are in a good agreement with the results of [17]. Fig. 17 shows the variation of stiffness coefficient Ksr with eccentricity ratio for different values of aspect ratio. This figure shows that Ksr values are increased with the increase of eccentricity ratio value for the case of aspect ratio equal (0.5) only, while for the cases of aspect ratio equal (1 and 1.5), Ksr values are decreased slightly in the range (0 – 0.3) for eccentricity ratio and then increased. It also shows that, the relation between the aspect ratio and Ksr is proportional. These results are in a good agreement with the results of [17].

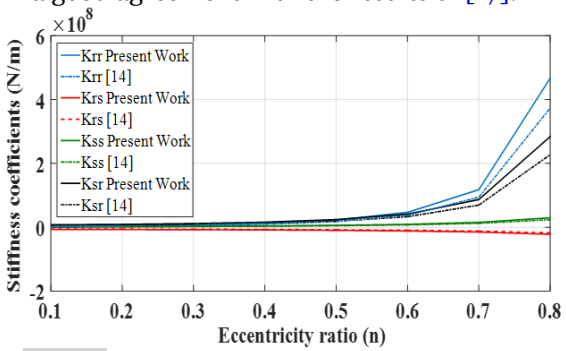

Fig. 2. Stiffness coefficients vs. eccentricity

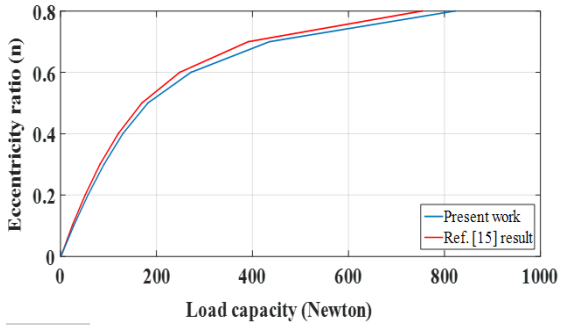

Fig. 3. Load capacity vs. eccentricity ratio (for elliptical bearing)

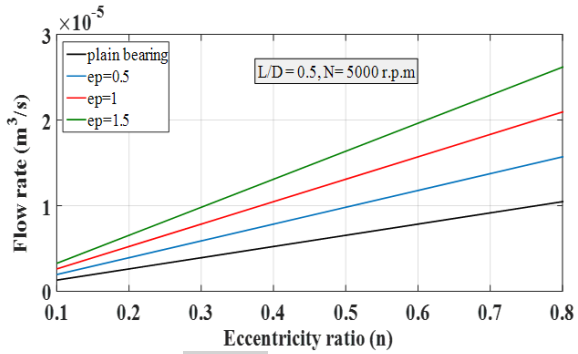

Fig. 4. Q_r Vs. n

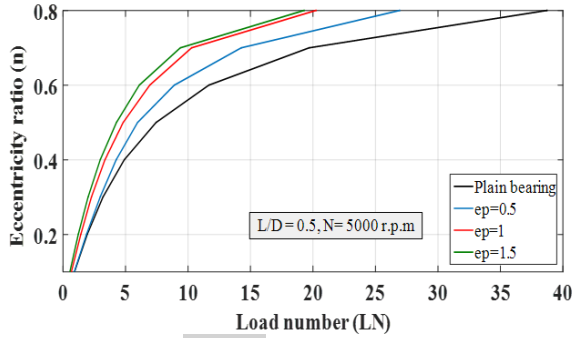

Fig. 5. L_N Vs. n

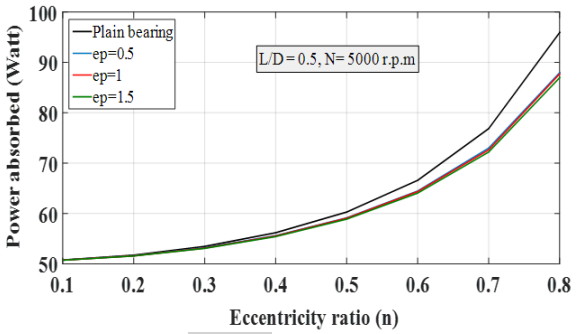

Fig. 6. ψ Vs. n

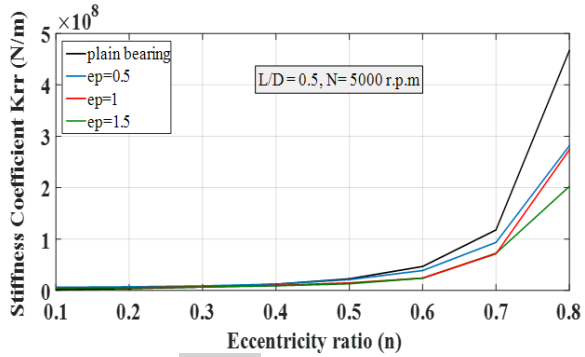

Fig. 7. Krr Vs. n

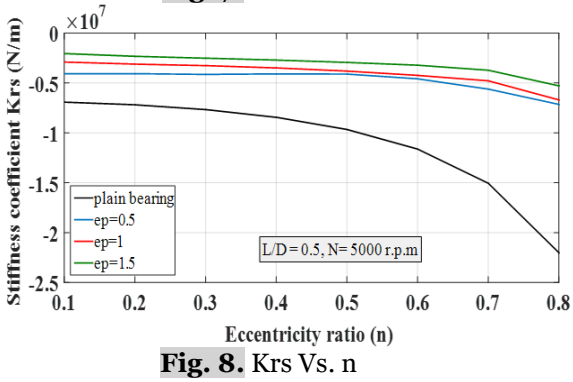

Fig. 8. Krs Vs. n

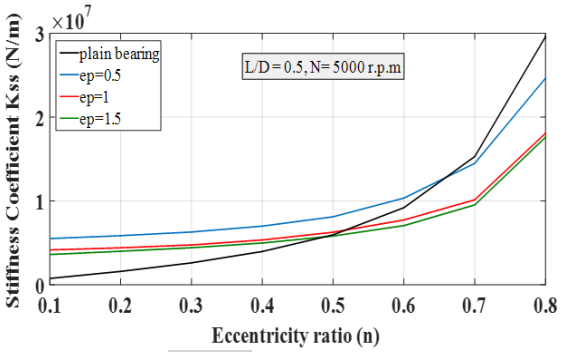

Fig. 9. Kss Vs. n

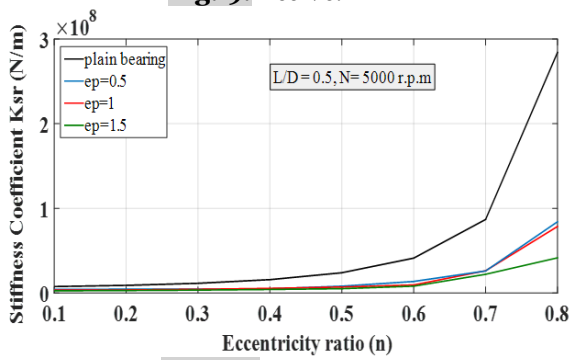

Fig. 10. Ksr Vs. n

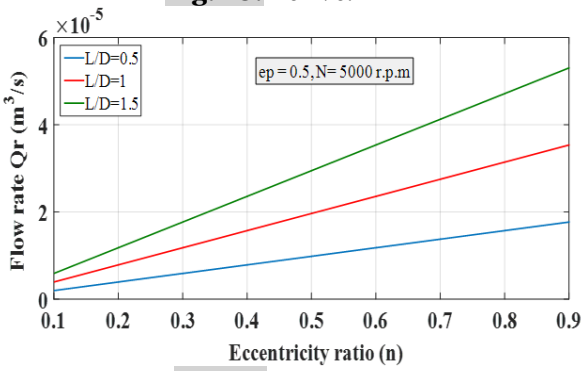

Fig. 11. Q_r Vs. n

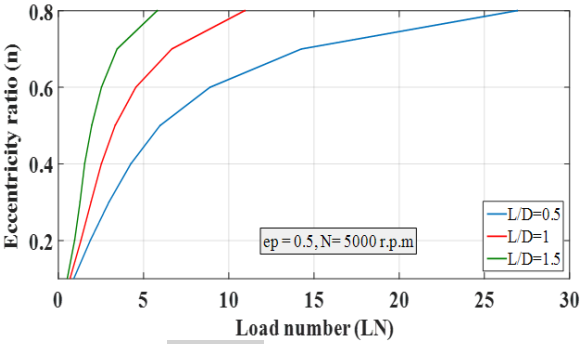

Fig. 12. L_N Vs. n

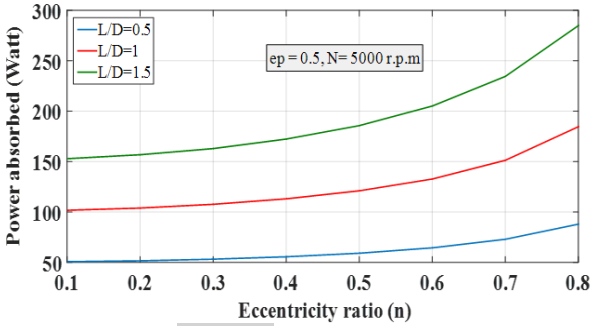

Fig. 13. ψ Vs. n

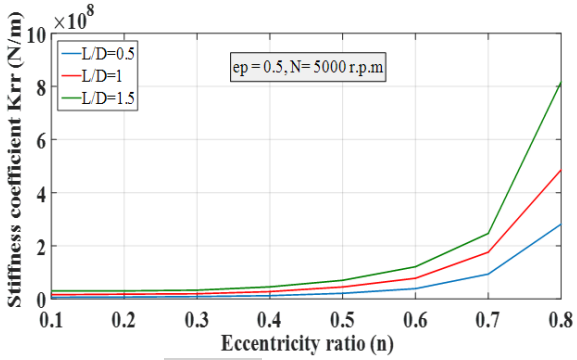

Fig. 14. Krr Vs. n

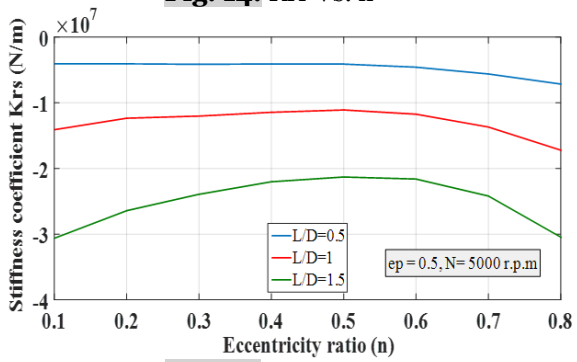

Fig. 15. Krs Vs. n

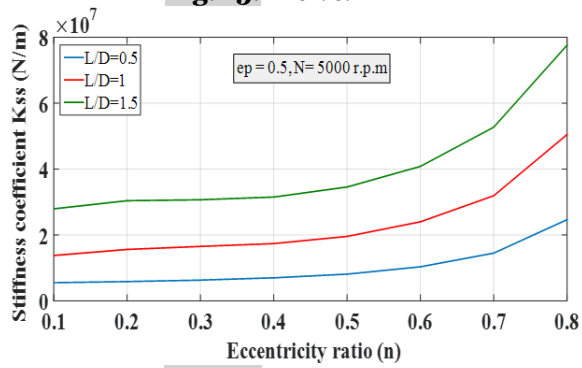

Fig. 16. Kss Vs. n

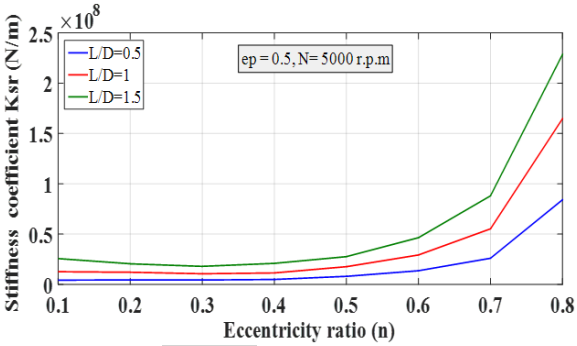

Fig. 17. Ksr Vs. n

4.CONCLUSIONS

The following conclusions are obtained from this study:

1. The elliptical bearing has high values of flow rate and fewer values of (load capacity and power losses) than the conventional bearing.
2. The elliptical bearing has high values of principle stiffness coefficients (Krr and Kss) in the region (n<0.41) and (n<0.66), respectively, and fewer values of cross-coupling stiffness coefficients (Krs and Ksr) than the conventional bearing.

3. Increasing the ellipticity ratio gives an increase in the flow rate values and a decrease in the (load number, power losses, Krr, Kss, |Krs| and Ksr) values.

Increasing the aspect ratio (L/D) gives an increase in the (flow rate, power losses, Krr, Kss, |Krs| and Ksr) values and a decrease in the load number values.

NOMENCLATURES

a = Semi-major axis of the bearing, Fig. 1
a_e = The area of each element on the bearing surface m^2
A = Bearing surface area m^2
b = Semi-minor axis of the bearing, Fig. 1
C_{max} = Horizontal radial clearance $(C_{max} = a - R)$ m, Fig. 1
C_{min} = Vertical radial clearance $(C_{min} = b - R)$ m, Fig. 1
D = Journal diameter m, Fig. 1
e = Eccentricity m, Fig. 1
e_p = Ellipticity ratio, $\left(e_p = \frac{C_{max} - C_{min}}{C_{min}}\right)$
$F_{\parallel}$ = Parallel component of the oil film force N, Fig. 1
$F_{\perp}$ = Perpendicular component of the oil film Force N, Fig. 1
h = Oil film thickness m, Fig. 1
i, j = Grid counter in the circumferential and axial directions respectively
k = Total number of grids along the bearing length (axially)
K_{ss} = Principal stiffness coefficient (the force and displacement are in the s-axis direction N/m
K_{sr} = Cross-coupling stiffness coefficient (the force is the s -axis direction and the displacement is in the r – axis direction N/m
L = Bearing length m , Fig. 1
L_N = Load Number
m = Total number of grids around the bearing (circumferentially), Fig. 1
N = Journal rotating speed $r.p.m$
$\bar{N}$ = Journal rotating speed $r.p.s$
n = Eccentricity ratio, $n = e/C_V$
P = Generated pressure in the oil film Thickness p_a
$\bar{P}$ = Specific pressure p_a, $\bar{P} = W/LD$
P_b = Bearing perimeter m
Q_r = Oil flow rate m^3/s
R = Journal radius m, Fig. 1
r, s = (Bearing coordinates system) parallel and perpendicular axes to the line of centers, Fig. 1
U_o = Linear velocity of the journal m/s, $U_o = \pi D\bar{N}$
W = Load carrying capacity of the bearing N, Fig. 1
z = Axial Coordinate, Fig. 1
ϕ = Attitude angle $deg.$, Fig. 1
$\Delta\theta$ = Increment in the θ-direction $deg.$
ψ = Power absorbed $watt$
θ = Circumferential coordinate, Fig. 1
K_{rr} = Principal stiffness coefficient (the force and displacement are in the r-axis direction) N/m
K_{rs} = Cross-coupling stiffness coefficient (the force is in the r -axis direction and the displacement is in the s -axis direction) N/m
Δz = Increment in the z-direction m
μ = Dynamic viscosity of the lubricant $p_a.s$
ω = Angular velocity of the rotating shaft, rad/s, Fig. 1

REFERENCES

[1] Shubat HN. **Study the Effect of the Foundation Material on the Stiffness Coefficients of the Hydrodynamic Bearing**. University of Tikrit, Mech. Eng. Dep. (2019).

[2] Singh DV, Sinhasan R, Kumar A. A Variational Solution of Two Lobe Bearings. *Mechanism and Machine Theory*, 1977; **12**(_): 323-330.

[3] L. San Andres "an overview of tilting pad journal bearing. Texas A and M university, (2000).

[4] Crosby WA, Chetti B. **The Static and Dynamic Characteristics of a Two-lobe Journal Bearing Lubricated with Couple-Stress Fluid**. *Tribol. Trans.*, (2009), **52**(2), 262-268.

[5] Faria, Marco TC. **Finite Element Analysis of Oil-Lubricated Elliptical Journal Bearings**. *Inter. J. Mech.*, Aerosp, Indus. Mechatronic Manuf. Engin., 2015; **9**(5): 705-710.

[6] Awasthi RK, Sharma S. **Effect of Aspect Ratio on the Performance and Stability of Hydrodynamic Journal Bearings**," *Inter. J. Adva. Rese. Innov.*, 2016; **4**(1): 96-105.

[7] Hiromu H, **Dynamic Characteristic Analysis of Short Elliptical Journal Bearings in Turbulent Inertial Flow Regime**. *Tribol. Trans.*, 1992; **35**(4): 619-626.

[8] Atteaa MO. **Studying Effect of Pads Number on the Stiffness Coefficient of the Hydrodynamic Journal Bearing**.

University of Tikrit, Mech. Eng. Dep., (2017).

[9] Wu G, Wei X, Wang L, Zhou W. **A Superlinear Iteration Method for Calculation of Finite Length Journal Bearing's Static Equilibrium Position**. R. Soc. Open Sci. (RSOS), (2017), 4(5).

[10] Singh AP, Bagci C., "Hydrodynamic Lubrication of Finite Slider Bearings: Effect of One Dimensional Film Shape, and their Computer Aided Optimum Designs," ASME, (1983), 105(1), 48- 63.

[11] I. Ali Muhsin, 2"Design and evaluation of novel fluid film journal bearing", ph. D. thesis, Cranfield University, United Kingdom, (1991), Ch. 5, 14-16.

[12] Erik Oberg, Franklin D. Jones, Holbrook L. Horton, and Henry H. Ryfeel "Machinery's Handbook," Industrial Press, 29th Edition, (2012), 48- 50.

[13] John Wiley, Cameron A., Sons, "Basic Lubrication Theory," Second Edition, (1976), 22-25.

[14] M. J. Goodwin, P. J. Ogrodnik, M. P. Roach and Y. Fang, "Calculation and Measurement of the Stiffness and Damping Coefficients for a Low Impedance Hydrodynamic Bearing," J. Tribol. (1997), 119(1), 57-63.

[15] H. B. Sharda, H. N. Chandrawat and R. C. Bahl, "EHD Analysis of an Elliptical Bearing Using a Non- Conforming Finite Element Technique," Tribol. Inter., (1992), 25(2).

[16] I. Ali M. R., P. Medar & R. H. Malcolm E, "A Review on Non-Circular Hydrodynamic Bearing." Ind. Sci., (2014), 1(4), 1-7.

[17] S. C. Soni, R. Sinhasan and D. V. Singh, "Performance Characteristics of Noncircular Bearings in Laminar and Turbulent Flow Regimes," ASLE Trans., (1981), 24(1), 29-41.